

Article

Effects of Model Spatial Resolution on Ecohydrologic Predictions and Their Sensitivity to Inter-Annual Climate Variability

Kyongho Son ^{1,*}, Christina Tague ² and Carolyn Hunsaker ³

¹ Research Foundation of the City University of New York, New York, NY 10036, USA

² Bren School of Environmental Science & Management, University of California Santa Barbara, Santa Barbara, CA 93117, USA; ctague@bren.ucsb.edu

³ Pacific Southwest Research Station, USDA Forest Service, Fresno, CA 93710, USA; chunsaker@fs.fed.us

* Correspondence: kkyong77@hotmail.com; Tel.: +1-805-570-8553

Academic Editors: Christopher J. Duffy and Xuan Yu

Received: 9 May 2016; Accepted: 15 July 2016; Published: 29 July 2016

Abstract: The effect of fine-scale topographic variability on model estimates of ecohydrologic responses to climate variability in California's Sierra Nevada watersheds has not been adequately quantified and may be important for supporting reliable climate-impact assessments. This study tested the effect of digital elevation model (DEM) resolution on model accuracy and estimates of the sensitivity of ecohydrologic responses to inter-annual climate variability. The Regional Hydro-Ecologic Simulation System (RHESys) was applied to eight headwater, high-elevation watersheds located in the Kings River drainage basin. Each watershed was calibrated with measured snow depth (or snow water equivalent) and daily streamflow. Modeled streamflow estimates were sensitive to DEM resolution, even with resolution-specific calibration of soil drainage parameters. For model resolutions coarser than 10 m, the accuracy of streamflow estimates largely decreased. Reduced model accuracy was related to the reduction in spatial variance of a topographic wetness index with coarser DEM resolutions. This study also found that among the long-term average ecohydrologic estimates, summer flow estimates were the most sensitive to DEM resolution, and coarser resolution models overestimated the climatic sensitivity for evapotranspiration and net primary productivity. Therefore, accounting for fine-scale topographic variability in ecohydrologic modeling may be necessary for reliably assessing climate change effects on lower-order Sierra Nevada watersheds (≤ 2.3 km²).

Keywords: DEM resolution; ecohydrologic modeling; climate change effects; RHESys; California's Sierra

1. Introduction

In recent decades, warmer temperatures in the western United States have led to a reduction of snow accumulation as well as earlier melt and streamflow [1,2]. Changing snowmelt input has also altered the timing and magnitude of soil moisture, vegetation water use and productivity [3]. A variety of hydrological models have been used to assess the effect of climate change on the ecohydrologic response at various watershed scales [1,4,5]. However, spatial units in these models tend to be defined at relatively coarse spatial resolutions (>100 m) and thus ignore the fine-scale variation of topography. Particularly in mountain environments, substantial variation in topographic properties over relatively short spatial scales is observed, and the distribution of atmospheric forcing variables (radiation, temperature and precipitation), and local and lateral moisture are often related to this fine-scale variation in topography. Therefore, ignoring the fine-scale variation of mountain topography may result in poor predictions of ecohydrologic responses to climate change for small watersheds.

Previous studies have emphasized the importance of detailed topographic information for characterizing hydrologic and geomorphic properties of watersheds and obtaining accurate hydrologic and ecologic predictions [6–8]. Cline et al. [7] showed that the mean snow water equivalent (SWE) predictions using a 90 m digital elevation model (DEM) are different from the predictions obtained using a 30 m DEM in the Emerald Lake watershed in California. Zhang and Montgomery [6] showed that TOPMODEL [9] using a DEM with 10 m resolution improved streamflow predictions compared to simulations using coarser DEM (30 m and 90 m) for two small catchments in the western United States. Lassueur et al. [8] demonstrated the usefulness of a fine-resolution DEM to estimate plant species richness in an alpine landscape.

Studies evaluating the response of model performance to DEM resolution show that sensitivity varies across sites. Kuo et al. [10] showed that model estimates for slowly undulating landscapes tend to be less degraded with increasing grid size than those for landscapes with steep valleys. Their research also found that runoff does not change with grid size in wet years, but does change in dry years. Model predictions for snow-dominated watersheds may be more sensitive to DEM resolution than those for rain-dominated watersheds because topographic parameters (elevation, aspect and slope) determine the energy input, thereby controlling the snow melt patterns [11,12]. DEM resolution also affects the snow accumulation estimates because many snow models use a simple lapse rate based on air temperature and elevation to partition the total precipitation into snow and rain.

The effect of DEM resolution on model predictions also varied with the variable of interest [13]. Using Soil and Water Assessment Tool (SWAT) modeling, coarsened DEM resolution was found to reduce the accuracy of both streamflow and NO₃-N load prediction, but not the accuracy of total P load predictions [13]. A distributed hydrologic model used to predict average soil moisture and streamflow at the hillslope scale showed that using a coarser DEM did not reduce model accuracy, but the spatial pattern of soil moisture was distorted [14]. Estimates from a distributed ecohydrologic model showed that the grid-size effect on net primary productivity (NPP) estimates is more significant than on evapotranspiration (ET) estimates [15].

These previous studies have focused on the effect of DEM resolution on model predictions in general. However, the importance of fine-scale topographic variation in hydrologic modeling for climate change studies and other issues is not well understood. The declines in accuracy with coarsening resolution noted above may or may not be critical for using models to make inferences about climate change effects. Vegetation water and productivity are important variables for assessing the effect of climate change on ecosystem productivity, but previous hydrologic studies do not integrate the effect of DEM resolution on changes in water availability and the related impacts on modeled ET and NPP.

This study evaluated the effect of DEM resolution on the accuracy of modeled streamflow, specifically for rain-snow transition watersheds and snow-dominated watersheds that are expected to be particularly sensitive to climate change. This study also explicitly tested how DEM resolution influences the sensitivity of modeled ecohydrologic responses (annual streamflow, summer flow, annual ET and annual NPP) to inter-annual climate variability. Investigation of the influences of DEM resolution on the estimates of ecohydrologic responses to historic climate variability serves as an indicator of the likely importance of DEM resolution for future predictions.

The Regional Hydrologic-Ecologic Simulation System (RHESSys) [16] was applied to eight small Sierra Nevada watersheds. The watersheds have different dominant precipitation phases (snow vs. rain), topographic properties (elevation, slope and aspect), and vegetation properties (leaf area index, rooting depths). This study answers three questions: (1) does the total precipitation phase (snow vs. rain) control the sensitivity of model estimates to DEM resolution; (2) which topographic parameters determine the sensitivity of model estimates to DEM resolution; and (3) which variable of interest among model estimates is the most sensitive to DEM resolution? Model estimates consider both annual means and inter-annual variation in ecohydrologic variables. To answer these questions, this study follows the framework outlined in Figure 1. First, this study investigates the effect of DEM resolution

on topographic parameters (elevation, slope, aspect and wetness index) in the eight watersheds. Second, this study identifies the watershed sensitivity based on the difference in estimates of the snow water equivalent (SWE), and the accuracy of modeled daily streamflow among various resolution models. Finally, this study estimates the sensitivity of the model estimates of the four ecohydrologic variables (annual streamflow, summer streamflow, annual ET and annual NPP) to DEM resolution. These tests provide a guideline for determining the appropriate DEM resolution in ecohydrologic modeling for climate effect assessment for the Sierra Nevada watersheds.

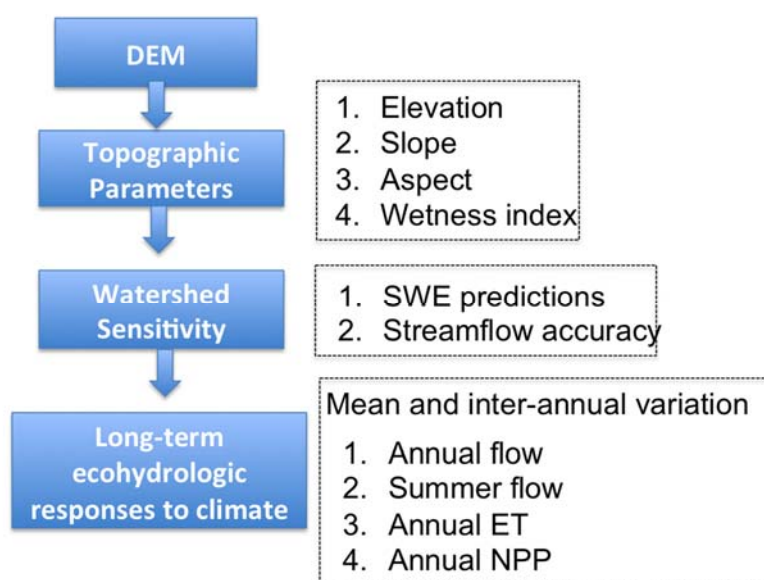


Figure 1. Framework for studying the effect of DEM resolution on the topographic parameters, the watershed sensitivity and the long-term ecohydrologic responses to climate in the eight Sierra Nevada watersheds.

2. Research Sites

This study site is located at the Forest Service's Kings River Experimental Watersheds (KREW) in California (Figure 2). RHESSys was implemented for gauged watersheds within the KREW Providence site (P301, P303, P304 and D102) and the Bull site (B201, B203, B204 and T003). Detailed descriptions of each watershed are provided below.

2.1. Providence Sites

The Providence sites include P301 (0.99 km²), P303 (1.32 km²), P304 (0.49 km²) and D102 (1.2 km²). Elevations range from 1485 m to 2115 m. The average annual precipitation (from the year 2002 to the year 2006) is 1350 mm. Precipitation occurs primarily in the winter as a mixture of snow and rain, and with little contribution of storm rainfall during the summer. In Providence sites, 20% to 50% of the annual precipitation falls as snow [17]. Following the snow regime classification developed by Jefferson [18], P301, P303, P304 and D102 are transient snow watersheds (TSWs). The major soil types are Shaver soil and Gerle-Cagwin soil [17]. The runoff ratio for the Providence sites ranges from 0.23 to 0.36. P304 has the largest runoff ratio at 0.36, and P303 has the lowest value at 0.23. The dominant forest type is Sierran mixed-conifer forest with some mixed chaparral and barren land cover. Sierran mixed-conifer vegetation in this location consists largely of white fir (*Abies concolor*), ponderosa pine (*Pinus ponderosa*), black oak (*Quercus kelloggii*), sugar pine (*Pinus lambertiana*) and incense cedar (*Calocedrus decurrens*). Two climate stations are located near or in the P303 watershed. A station is located near the outlet of the P303 watershed, while the other station is at the top of the P303 watershed. At the two stations, hourly precipitation, minimum and maximum air temperature,

relative humidity, solar radiation, wind speed and direction and snow depth have been measured since 2002. The snow depth data are collected using acoustic snow-depth sensors (Judd Communications TM LLC). At the upper climate station, SWE is measured with snow pillows (Mendenhall Manufacturing, McClellan, CA, USA). Each watershed has two flumes at the outlet to measure low and high flows.

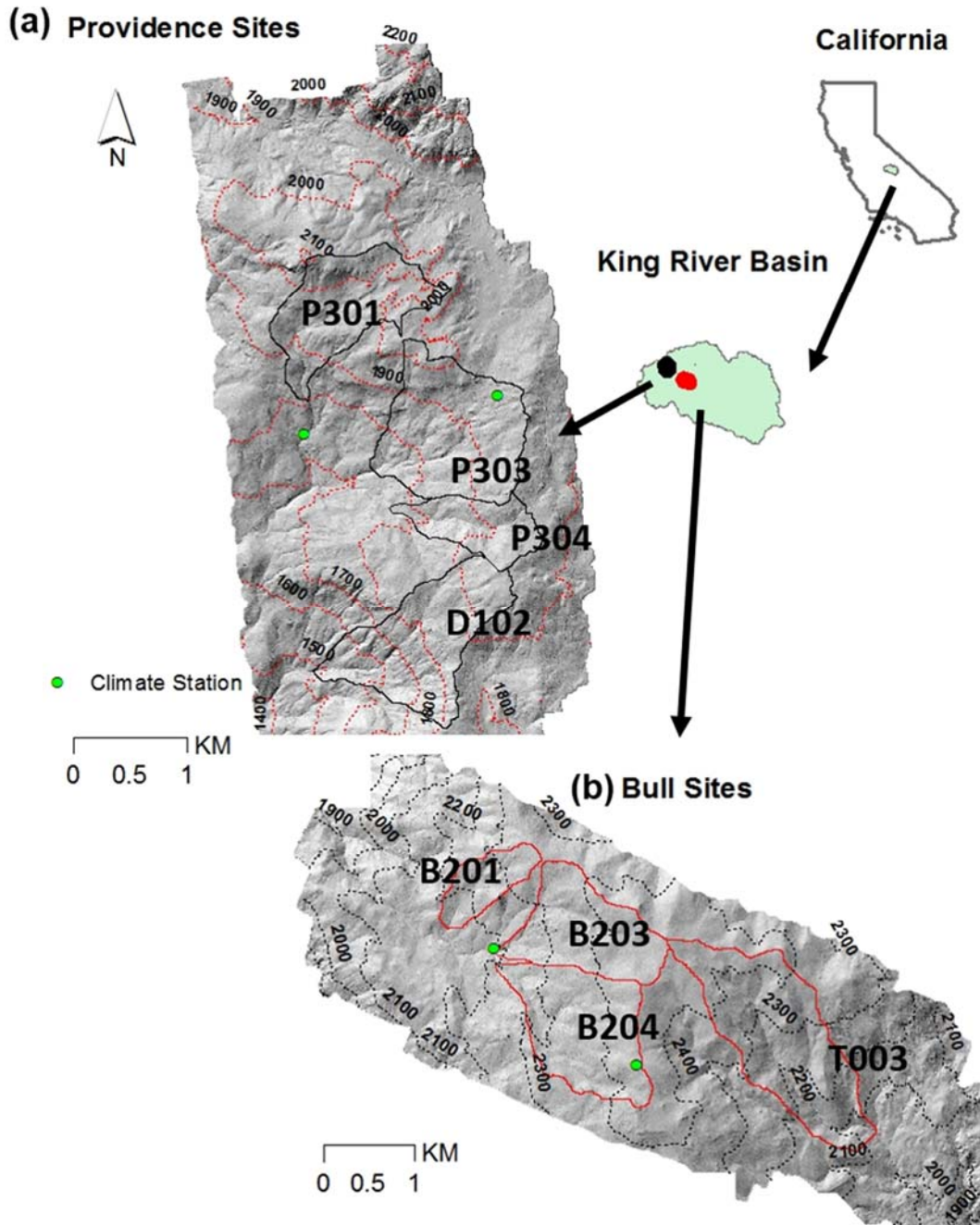


Figure 2. The location of climate stations, streamflow gauge stations and elevation gradient of study sites: (a) Providence sites and (b) Bull sites.

2.2. Bull Sites

The Bull sites include B201 (0.53 km²), B203 (1.4 km²), B204 (1.7 km²) and T003 (2.3 km²). Elevations range from 2050 m to 2490 m. The average annual precipitation (from the year 2003 to the year 2007) is 1300 mm. The Bull site is more snow-dominated (75% to 95% of precipitation

falls as snow) than the Providence site. B201, B203, B204 and T003 are classified as snow-dominated watersheds (SDWs). The runoff ratio for the Bull sites ranges from 0.36 to 0.53. The runoff ratio values for the Bull sites are larger than those for the Providence sites. B203 has the largest runoff ratio at 0.53, and T003 and B201 have the lowest value at 0.36. The major soil type is Cagwin soil [18]. Similar to the Providence site, the dominant forest type in the Bull site is Sierra mixed conifer; however, red fir (*Aibes magnifica*) is more dominant at this elevation than white fir. Two climate stations are located near or in the B204 watershed. The lower climate station is located near the outlet of the B204 watershed, while the upper station is located at the top of the watershed. The station measures the same meteorological variables as at the Providence meteorological stations, and the meteorological data has been collected since year 2003. Each watershed has two flumes at the outlet of the watershed to measure high and low flow, and streamflow has been measured since 2003. A detailed description of measurements and instruments is provided by Hunsaker et al. [17].

3. Methodology

3.1. Effect of DEM Resolution on Topographic Parameters

This study tested the effect of the DEM resolution on topographic parameters including elevation, aspect, slope and topographic wetness index for the eight Sierra Nevada watersheds. The topographic wetness index [9] is defined as $\ln\left(\frac{a}{\tan\beta}\right)$, where a is the local upslope contributing area per unit contour length and $\tan\beta$ is the slope angle of the ground surface. Each DEM product was derived from a 1 m LIDAR DEM (available at <https://eng.ucmerced.edu/snsjho/files/MHWG/LiDAR>) with a bilinear interpolation algorithm. Providence and Bull site boundaries were derived from 5 m LIDAR DEM in order to minimize the effect of the DEM resolution on deriving the watershed area. However, due to the irregular edges, small differences in estimating the watershed area are unavoidable. Other topographic parameters including elevation, slope, aspect and wetness index were derived with five different resolutions (5 m, 10 m, 30 m, 90 m and 150 m).

The Wilcoxon rank-sum test was used to quantify the difference of the topographic parameters between the finest DEM (5 m) and other coarser DEM resolutions (10 m, 30 m, 90 m and 150 m) (Table 1). Values for topographic parameters were taken from each grid cell within the watershed boundaries. For all watersheds and for all DEM resolutions, the watershed mean values of slope and wetness index are significantly different (p -value < 0.01) from those computed using the 5 m resolution. However, coarsening the DEM generally does not influence the mean values of elevation and aspect except in few cases. For example, for two of Providence's transient snow watersheds (D102 and P304), the mean values of elevation using 10 m are significantly different (p -value < 0.05) than those computed using 5 m. Among the snow-dominated watersheds, B204's mean aspect values using 90 m and 150 m are significantly different (p -value < 0.1) from those computed using 5 m. T003 also has significantly different (p -value < 0.1, p -value < 0.01) mean values of aspect using 5 m compared with those computed using 10 m, and the resolution greater than 10 m, respectively.

Density plots were used to qualitatively compare the overall distributions of the topographic parameters. The density plots for only slope and wetness index parameters are presented in Figures 3 and 4 because these two parameters have the most significant change with coarsening DEM. In general, coarsening DEM decreases the mean of slope and its variation for all watersheds. Across all watersheds in the Bull and Providence sites, the largest difference in the distribution of slopes occurs between 5 m and 90 m, and between 5 m and 150 m resolutions; there is a similar distribution of slope between 5 m and 10 m, between 5 m and 30 m.

Table 1. The watershed mean values of topographic parameters with various digital elevation model (DEM) resolution (5 m, 10 m, 30 m, 90 m and 150 m) for the Providence sites and the Bull sites.

Watershed Mean Value of Topographic Parameters ¹						
Watershed	Parameter	DEM Resolution				
		5 m	10 m	30 m	90 m	150 m
P301	Elevation (m)	1975.9	1976.6	1976.7	1975.5	1982.1
	Slope (°)	12.3	11.9 ***	10.7 ***	9.2 ***	7.8 ***
	Aspect ² (°)	258.8	259.0	256.5	256.3	266.6
	Wetness (m)	5.9	6.2 ***	7.0 ***	7.8 ***	8.4 ***
P303	Elevation (m)	1894.8	1894.5	1895.4	1890.9	1901.7
	Slope (°)	14.0	13.7 ***	12.6 ***	11.6 ***	10.7 ***
	Aspect ² (°)	214.4	214.9	214.4	212.4	218.2
	Wetness (m)	6.0	6.5 ***	7.2 ***	7.8 ***	8.0 ***
P304	Elevation (m)	1898.1	1896.8 *	1898.1	1894.3	1905.5
	Slope (°)	13.8	13.5 ***	12.5 ***	10.7 ***	8.5 ***
	Aspect ² (°)	165.8	166.5	167.1	162.5	169.7
	Wetness (m)	5.9	6.2 ***	6.8 ***	7.7 ***	8.0 ***
D102	Elevation (m)	1772.0	1774.8 **	1772.8	1767.4	1785.4
	Slope (°)	19.2	18.6 ***	17.4	15.8 ***	14.8 ***
	Aspect ² (°)	200.8	200.9	200.8	199.6	203.4
	Wetness (m)	5.7	6.1 ***	6.9 ***	7.6 ***	7.7 ***
B201	Elevation (m)	2253.8	2253.7	2254.4	2251.9	2248.4
	Slope (°)	12.5	12.3 ***	11.7 ***	10.0 ***	9.3 ***
	Aspect ² (°)	217.2	217.2	215.8	215.4	214.8
	Wetness (m)	6.3	6.5 ***	6.9 ***	7.7 ***	7.9 ***
B203	Elevation	2371.9	2371.6	2372.4	2372.7	2369.6
	Slope	12.1	11.9 ***	11.3 ***	9.7 ***	8.3 ***
	Aspect	189.4	189.5	188.9	184.9	184.0
	Wetness	6.4	6.7 ***	7.2 ***	7.8 ***	8.0 ***
B204	Elevation	2360.3	2360.0	2360.7	2361.0	2357.3
	Slope	12.1	11.9 ***	11.1 ***	9.0 ***	8.2 ***
	Aspect	178.2	177.8	176.7	173.2*	172.6*
	Wetness	6.3	6.5 ***	7.0 ***	7.8 ***	8.4 ***
T003	Elevation	2286.5	2287.0	2285.8	2283.2	2292.8
	Slope	15.7	15.5 ***	14.5 ***	11.7 ***	9.7 ***
	Aspect	304.0	304.1 *	305.1 ***	309.3 ***	308.8 ***
	Wetness	6.0	6.2 ***	6.6 ***	7.4 ***	8.2 ***

Notes: ¹ Watershed-scale parameter values; ² Aspect is calculated with Grass GIS program (r.slope.aspect): 90° is North, 180° is West, 270° is South, and 360° is East. The aspect having zero is used to indicate undefined aspect in flat areas with slope having zero. *p*-value of Wilcoxon rank-sum test; Asterisks indicate a significant difference in mean values between the topographic parameters computed using the 5 m DEM and those using the coarser DEMs (* *p* < 0.1; ** *p* < 0.05; *** *p* < 0.01).

Coarsening the DEM increases the mean of the wetness index, but inconsistently changes the variance of the wetness index (Figure 4). The changes in the wetness index distribution with resolution are not linear and different resolutions often have different shapes of the wetness index distribution. TSWs and SDWs have a substantial change in the distribution of the wetness index at resolutions coarser than 10 m and 30 m, respectively. These results suggest that the DEM resolution may have a larger effect on local moisture estimates and lateral flow drainage patterns.

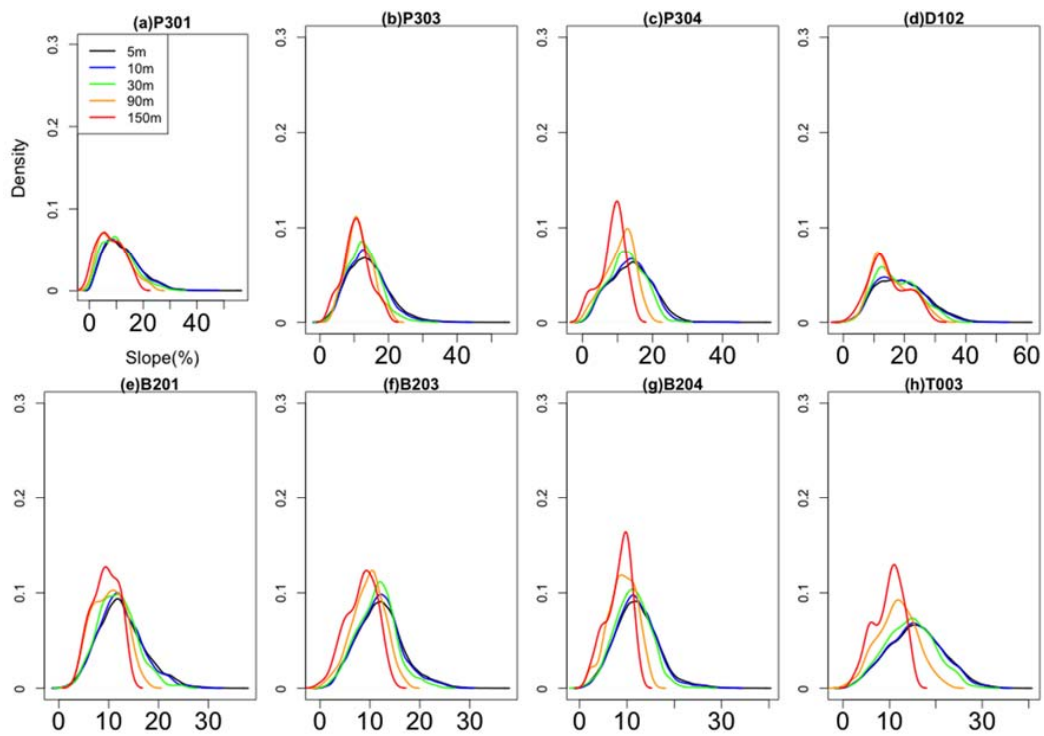


Figure 3. Distribution of slope computed using different DEM resolutions: (a) P301; (b) P303; (c) P304; (d) D102; (e) B201; (f) B203; (g) B204 and (h) T003. The first column displays the TSWs, and the second column displays the SDWs.

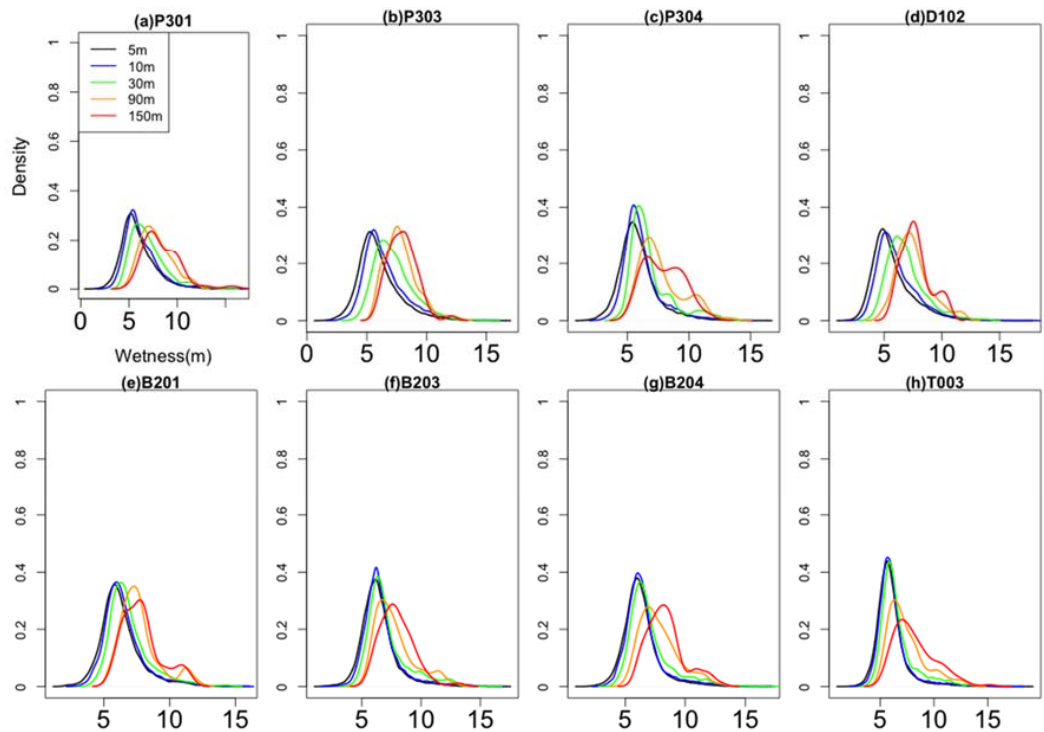


Figure 4. Distribution of wetness index using different DEM resolutions: (a) P301; (b) P303; (c) P304; (d) D102; (e) B201; (f) B203; (g) B204 and (h) T003. The first column displays the TSWs, and the second column displays the SDWs.

This study also estimated the watershed-scale mean and standard deviation of slope and wetness index computed using the different DEM resolutions (Figure 5). At 5 m, D102 and T003 have the largest mean slope of 19.2 and 15.7 for TSWs and SDWs, respectively. Among TSWs, P304 has the largest change in mean slope (5.3, 38%), and among SDWs, T003 has the largest change in mean slope (6.0, 38%) with different DEM resolutions. TSWs tend to have larger spatial variance of slope at 5 m than SDWs, but the change in the spatial variance of slope with coarsening DEM is similar between TSWs and SDWs. SDWs tend to have a larger mean wetness index at 5 m than TSWs, but TSWs tend to have larger spatial variance of wetness index at 5 m than SDWs. Among TSWs, the spatial variances of the wetness index for P303 and D102 tend to decrease with coarsening DEM. Their variances for P301 and P304 increase with coarsening resolution up to 30 m, and their variances decrease at 90 m and 150 m, respectively. Among SDWs, the spatial variances of wetness index for B203 and B204 increase for resolutions up to at 30 m, and then decrease. Spatial variance of the wetness index for B201 slightly decreases with coarsening DEM. However, its variance for T003 increases with coarsening DEM. In summary, increasing the DEM resolution generally decreases the mean and standard deviation of the slope, and increases the mean wetness index for all watersheds. The changes in the standard deviation of the wetness index with coarsening the DEM have more complex patterns than other parameters.

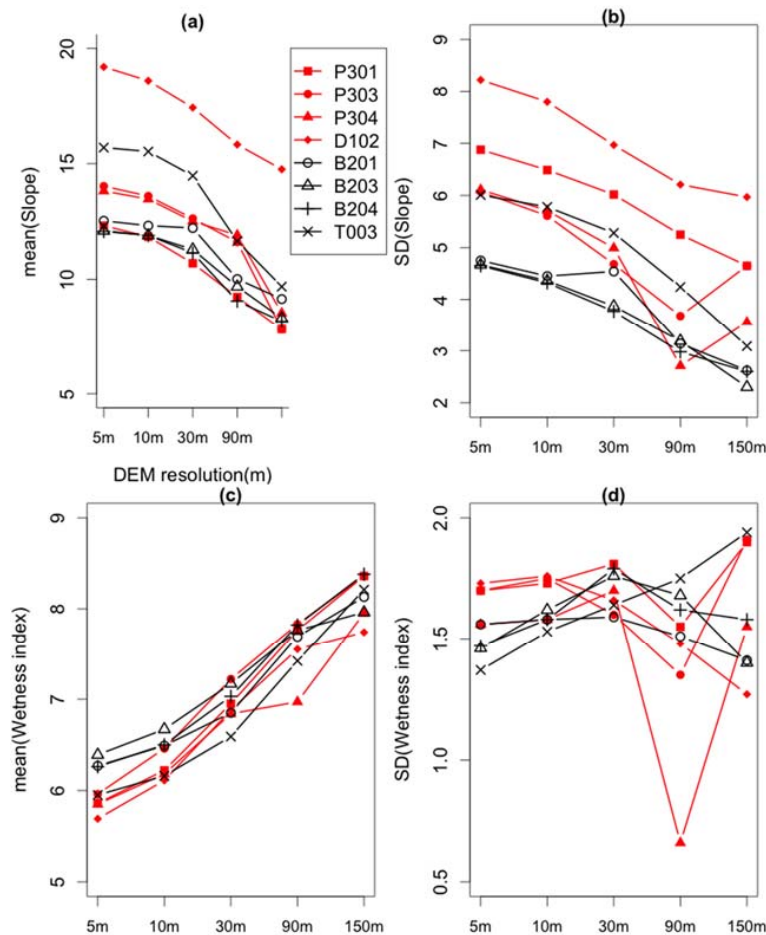


Figure 5. Watershed-scale statistical properties (mean and standard deviation) for slope and wetness index in the eight Sierra Nevada watersheds computed with increasingly coarse DEM resolution. (a) watershed mean values of slope; (b) watershed standard deviation of slope; (c) watershed mean values of wetness index; and (d) watershed standard deviation values of wetness index. Red color line refers to TSWs; black color line refers to SDWs.

3.2. Model Description

The RHESSys [16] was used to investigate the effect of DEM resolution on the model estimates of ecohydrologic fluxes of the eight small Sierra Nevada watersheds in California. The RHESSys is a physically-based, distributed ecohydrologic model. The RHESSys is under continuous development. In this study, version 5.15.r326 was used. A detailed description of the model is provided in [16].

The RHESSys has a hierarchic spatial structure to partition the landscape: basins, hillslope, zones, patches and canopy strata. Patch and canopy strata are the smallest spatial units, and these can be derived using various layers: landcover, soil and elevation maps. In this study, a patch was defined as a grid cell with uniform elevation. Hydrological variables including snow, soil moisture and evapotranspiration are computed at the patch level. Within a patch, multiple horizontal and vertical canopy layers can be potentially used, but in this study we used a simple, single, vertical-layer canopy strata with the same horizontal (spatial) resolution as the patch. In addition to a canopy layer, patches also contain a litter layer. Zones were used to characterize the spatial and temporal distribution of climate inputs including precipitation, air temperature and solar radiation. To account for the fine-scale variability of the climate within a watershed, we defined zones using the same spatial data (elevation grids) that are used to define the patches. In the RHESSys, basins are the largest spatial unit, and it is generally defined as a hydrologically closed drainage area. In this study, the basins were created based on the stream gauging station, using *r.water.outlet* (GRASS GIS, (<http://grass.osgeo.org/>)). Hillslope maps were created using *r.watershed*, and the multiple flow direction algorithm [19] was used to create the flow direction maps, and a hillslope drains a single stream reach. Lateral flow is organized within a hillslope, and is computed at the patch level.

The minimum climate data required for model simulation include daily precipitation, and daily maximum and minimum air temperature data. Other climate data (including solar radiation, saturation vapor pressure, relative humidity, etc.) are computed using a climate interpolation model (MT-CLIM, Running et al. [20]). Mountain watersheds have frequently experienced a lack of available climate data usable for hydrologic modeling, largely due to high climate variability along steep topographic gradients. MT-CLIM has been tested and improved using field data, and has successfully reproduced the field measured climate data [21–23].

Energy, wind and water are attenuated through the aboveground canopy, using standard approaches such as Beer's Law for radiation extinction as a function of vegetation leaf area index. Snowmelt is estimated using a combination of an energy budget approach for radiation-driven melt and advective-driven melt (rain on snow) with a temperature index-based approach for sensible and latent heat exchange. The partitioning of total precipitation into snow versus rain is calculated based on linear temperature threshold values. Transpiration from the canopy and evaporation of intercepted water and soil evaporation are computed using the Penman-Monteith [24] approach, where stomatal conductance for vegetation is computed using a Jarvis multiplicative model of radiation, vapor pressure deficit, rooting zone soil moisture and temperature controls [25]. Net primary productivity is estimated as the difference between gross photosynthesis and respiration. Gross photosynthesis is estimated using the Farquhar model [26]. Respiration is computed separately for different plant components (leaves, live/dead wood and roots) as a function of biomass, nitrogen content and air temperature [27]. Infiltration and vertical drainage between unsaturated and saturated stores is a function of soil hydraulic parameters. A lateral shallow groundwater flux is calculated based on hydraulic gradients (determined by surface topography) and soil hydraulic conductivity, and is explicitly routed between patches. The explicit routing scheme is based on topographic slope and soil transmissivity. The model also includes a bypass flow mechanism to simulate direct drainage through macropores from surface to deep groundwater storage. The flow from deep groundwater storage is calculated based on a linear storage equation.

This study compared RHESSys estimates from model implementations using five different resolutions (5 m, 10 m, 30 m, 90 m and 150 m). For example, for RHESSys, the DEM is used to derive topographic parameters (elevation, aspect, slope and flow drainage parameter (e.g., wetness

index)) that determine the distribution of the microclimate (radiation, temperature, etc.), and local and lateral moisture distribution. Changing the DEM resolution is therefore expected to affect the RHESSy model estimates, including SWE, ET, NPP and streamflow. Each resolution model had the same vegetation definition map. The vegetation type for all watersheds was assigned as mixed conifer. Associated vegetation type parameters were taken from RHESSys parameter libraries (<http://fiesta.bren.ucsb.edu/~rhessys/index.html>). Leaf area index (LAI) was derived from the LIDAR point cloud using a deterministic approach [28] and was used to initialize vegetation carbon and nutrient stores. To minimize the effect of LAI resolution on model estimates, 30 m LAI was used for all resolution models. We recalibrated the model for each DEM resolution—thus, each resolution has a unique set of parameters. We chose this option, rather than running with the same parameterization, because this better reflects how models are typically implemented—and the focus of the paper is exploring how model implementations (which include calibration) influence estimates. While in this paper we focus on differences in model estimates based on an optimal parameter set, we note, however, that the different resolutions may also be associated with differences in parameter uncertainty.

3.3. Model Calibration

We used a 5 m resolution model as a baseline model. Snow-related parameters were estimated by comparing model SWE predictions of the 5 m resolution model with measured snow depths (or measured SWE) at the climate stations. Table 2 shows estimated air temperature and snow-related parameters for the Providence and the Bull sites. The two climate stations are located at the top and bottom of the watersheds, respectively. Thus, air temperature lapse rates for the Providence and Bull sites were estimated using the difference of the elevations and the difference of the measured air temperatures at the two climate stations, respectively. Positive lapse rates for maximum daily temperature and negative lapse rates for minimum daily temperature are obtained for both sites. Since the climate stations (Lower Providence and Lower Bull) at lower elevations are located in a valley or a potential cold pool drainage area, the measured air temperature data at the station may reflect the nighttime temperature inversion. The two snow-related parameters, the temperature melt coefficient and the temperature threshold value for the partitioning of total precipitation into rain and snow, were estimated by adjusting the parameter values until the model prediction was similar to the measured snow depth or SWE. The Providence and Bull sites have similar temperature lapse rates and the same temperature melt coefficients and temperature threshold values. To compare the model estimate of the SWE and measured snow depths, the day of complete snowmelt in the four climate stations was calculated (Table 2). Model estimates were compared to measurements taken by acoustic snow-depth sensors. The model reproduces the timing of observed snowmelt at the four climate stations. The comparison of the model estimates with measured values results in R^2 values of 0.92, 0.86 in the Providence stations and the Bull stations. The comparison of the modeled SWE with measured SWE at the Upper Providence and the Upper Bull stations results in R^2 values of 0.91 and 0.83, respectively. In general, the model accuracy for SWE estimation is slightly better at the Providence station (transient snow watersheds) than at the Bull station (snow-dominated watersheds).

After snow-related parameters were estimated, soil parameters were calibrated by comparing daily estimates of model streamflow to measured streamflow. The calibrated soil parameters are anisotropic horizontal and vertical saturated hydraulic conductivity (K_{sat_h} , K_{sat_v}), the decay coefficient of saturated hydraulic conductivity with depth (m), the proportion coefficient of macro-pore drainage into deep groundwater storage (gw1), air entry pressure (ae) and pore size index (psi). The linear coefficient of deep groundwater storage (gw2) is fixed as zero to reflect deep groundwater losses that are not captured by the stream gauge. In addition, to account for the observed difference of the rooting depth across watersheds, Providence watersheds are assigned a 2 m rooting depth, and Bull watersheds are assigned a 1 m rooting depth [17].

Table 2. Calibrated snow-related parameters and the model accuracy of snow predictions for the Providence and Bull watersheds.

Watershed	Snow-Related Parameters			Model Accuracy of Snow Predictions	
	Temperature Lapse Rates ¹ (tmax/tmin) (°C/m)	Temperature Threshold for Rain vs. Snow ² (°C)	Temperature Melt Coefficient ³ (m/°C)	Day of Snow Melt ⁴	SWE ⁵
Providence	0.0063/−0.0064	−3-3	0.005	0.92	0.91
Bull	0.0068/−0.0060	−3-3	0.005	0.83	0.83

Notes: ¹ Since fine-spatial-scale air temperature is not available in the two watersheds, air temperature within a watershed is spatially interpolated with the given elevation and the calculated temperature lapse rates; ² To partition total precipitation into snow and rain, we use the air temperature as a proxy variable, and the proportion of snow and rain in the total precipitation is linearly interpolated based on the minimum and maximum temperature values; ³ Temperature melt coefficient accounts for snowmelt due to latent heat and sensible heat; ⁴ The day of snowmelt is estimated using observed snow depths and the modeled SWE value, and the correlation coefficient is measured; ⁵ The measured SWE data are available in the upper Providence and upper Bull station.

To evaluate the model streamflow accuracy, this study adopted a multi-objective approach. Many hydrologic modeling studies have found that using a single accuracy measure can bias the evaluation of the model performance [29]. This study's accuracy measures are listed in Equations (1)–(4). Each measure focuses on a particular aspect of flow variation. Nash-Sutcliffe efficiency (NSE) [30] focuses on peak streamflow. Log Nash-Sutcliffe efficiency (LNSE) is the log value of the Nash-Sutcliffe efficiency and focuses on recession and low flow. Percent Error (PerErr) is the percent volume error and focuses on flow bias. The three accuracy measures are combined to evaluate the model streamflow accuracy robustly (Equation (4)). This accuracy measure ranges from 0 to 1 with 1.

$$NSE = 1 - \frac{\sum_i (Q_{obs,i} - Q_{sim,i})^2}{\sum_i (\overline{Q_{obs}} - Q_{sim,i})^2} \quad (1)$$

$$LNSE = 1 - \frac{\sum_i (\log(Q_{obs,i}) - \log(Q_{sim,i}))^2}{\sum_i (\log(\overline{Q_{obs}}) - \log(Q_{sim,i}))^2} \quad (2)$$

$$PerErr = \frac{(\overline{Q_{obs}} - \overline{Q_{sim}})}{\overline{Q_{obs}}} \quad (3)$$

$$Total\ Accuracy = NSE \times LNSE \times PerErr \quad (4)$$

where $Q_{obs,i}$ is the observed streamflow and $Q_{sim,i}$ is the simulated flow at daily time step (i), and $\overline{Q_{obs}}$, $\overline{Q_{sim}}$ are the long-term average of observed daily streamflow and simulated streamflow, respectively.

Mean annual values for each flux (flow, ET and NPP) were computed to quantify the long-term average ecohydrologic responses to climate. The coefficient of variation (COV) was also calculated to quantify the inter-annual variation of each flux for climate sensitivity. The sensitivity of the mean and COV for each flux to DEM resolution was calculated. A long-term historical climate period (>50 years) is required to investigate the sensitivity of model estimates to inter-annual climate variability. However, at the time of this study the KREW streamflow and basic climate data were relatively short, just five years. Therefore, this study used the long-term climate data of the Grant Grove station located 28 km south of the Bull sites. The Grant Grove station has similar temporal precipitation and temperature patterns to the Providence and the Bull climate stations. The long-term climate data for the Providence and the Bull climate stations were estimated by fitting the local climate station data to the Grant Grove station data. The mean annual precipitation of the Bull and Providence stations for the period of 2003 to 2007 and 2002 to 2006, respectively, was divided by the mean annual precipitation of the Grant Grove station in order to estimate precipitation scaling factors for each station. To generate long-term daily precipitation data for the Providence and the Bull stations, the respective precipitation scaling factor

(1.22 and 1.21) was applied to the Grant Grove station's daily precipitation data. To generate long-term daily maximum and minimum air temperature data for the two watersheds, linear regression models were estimated by fitting the local temperature data from the Providence and Bull climate stations to the Grant Grove station's climate ($0.73 < R^2 < 0.89$).

3.4. Effect of DEM Resolution on Model Accuracy and Long-Term Ecohydrologic Responses to Climate

This study tested the effect of DEM resolution on the accuracy of modeled streamflow (Equations (1)–(4)), and on the sensitivity of estimated ecohydrologic response to inter-annual climate variability. Three hypotheses were developed with respect to differences in the sensitivity of the model estimates to DEM resolution for transient snow watersheds (TSWs) and snow-dominated watersheds (SDWs). The first hypothesis is that the flow estimates for TSWs are more sensitive to DEM resolution than the flow estimates for SDWs. The underlying assumption for this hypothesis is that TSWs may have a larger change in precipitation phase (snow vs. rain) with the changing spatial resolution of DEM because TSWs more frequently experience air temperature close to 0 °C (threshold temperature, Table 2) than SDWs. The change in precipitation phase affects snow accumulation, which influences melt rates and streamflow estimates. Flow estimates in TSWs therefore will be more sensitive to DEM resolution than flow estimates in SDWs. The second hypothesis is that the change in the spatial variance of the wetness index is the dominant topographic parameter that determines the flow sensitivity to the DEM resolution. When the DEM resolution is coarser, a large change in the spatial variance of the wetness index for the eight watersheds was observed (Figure 5d). Even though RHESys does not use the wetness index directly for calculating the flow, change in the spatial variance of the wetness index with a coarsening DEM may reflect the influence of DEM resolution on the flow network in RHESys and ultimately the accuracy of flow estimates [31].

This study also compared the sensitivity of four key ecohydrologic estimates to DEM resolution—annual streamflow, summer streamflow (August flow), annual ET and annual NPP. The third hypothesis is that the sensitivity of the annual and summer streamflow estimates is more sensitive to DEM resolution than annual ET and NPP estimates. Here it is assumed that flows are controlled by topographic variation; the dominant controls of ET and NPP are climate and vegetation properties.

4. Results

4.1. Effect of DEM Resolution on Snow Predictions

To evaluate the effect of DEM resolution on SWE estimates, we calculated the watershed-scale peak SWE at the five different resolutions and the mean absolute difference in the watershed-averaged daily SWE estimates between the 5 m resolution and other coarser resolutions (Figure 6). Peak SWE across the watersheds ranges from 303 mm to 607 mm for the 5 m resolution model. The change in peak SWE estimates between the different resolutions is always less than 3% (Figure 6a). The mean absolute difference in the watershed-averaged SWE between 5 m and other coarser resolutions varies between watersheds (Figure 6b). The differences range from 0.3 to 4.5 mm. Their difference is relatively indistinguishable compared with the peak SWE that ranges from 303 mm to 608 mm. Therefore, the difference in SWE change with coarsening DEM is minor for the eight watersheds.

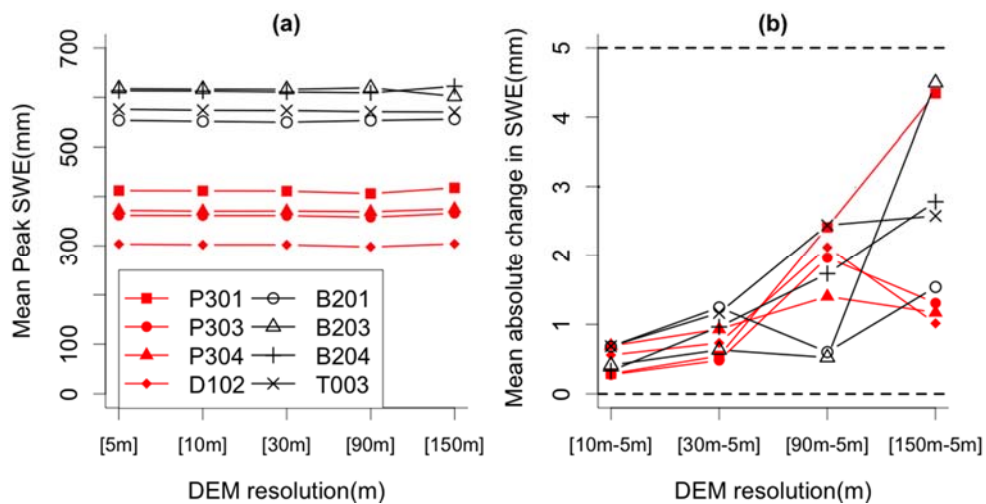


Figure 6. Watershed peak SWE estimates among various resolution and absolute difference in watershed mean SWE estimates between the 5 m resolution and the coarser resolutions (10 m, 30 m, 90 m and 150 m) in the eight Sierra Nevada watersheds. (a) watershed peak SWE; and (b) the difference in mean absolute watershed SWE estimates between 5 m and coarser resolutions.

4.2. Effect of DEM Resolution on Streamflow Prediction Accuracy

To quantify the effect of DEM resolution on streamflow predictions, we calculated the change in the four different streamflow accuracy measures with coarsening the DEM and compared the change in the streamflow accuracies between the eight watersheds. Figure 7 shows that the model accuracies declined with coarsening DEM resolutions for all watersheds. In general, there is a threshold resolution (10 m) above which coarser resolutions have a larger effect on streamflow prediction accuracy. Among TSWs, P304 and D102 equally have the largest reduction in streamflow total accuracy (Equation (4)) from 0.30 to 0.09 (71%) between 10 m and 30 m, and from 0.30 to 0.09 (71%) between 5 m and 90 m, respectively. P301 has the smallest reduction in streamflow accuracy (Equation (4)) from 0.48 to 0.36 (25%) between 5 m and 90 m. Among SDWs, B203 has the largest reduction in streamflow accuracy from 0.64 to 0.29 (55%) between 5 m and 150 m. T003 has the smallest reduction in streamflow accuracy (Equation (4)) from 0.55 to 0.47 (15%) between 10 m and 90 m. In general, streamflow estimates for the SDWs are more accurate and less sensitive to coarsening DEM resolution than the TSWs are.

Among the accuracy measures, PerErr changes most with coarsening DEM compared to the other individual measures (Figure 7b–d). The high sensitivity of PerErr may reflect the model error due to the impact of resolution on evapotranspiration estimates. LNSE values for most watersheds are least sensitive to DEM resolution (Figure 7c). NSE values for the TSWs are more sensitive to changes in DEM resolution than NSE values for the SDWs (Figure 7b). Among TSWs, NSE and LNSE values for P301 are the least sensitive to DEM resolution. The streamflow estimates for P304 are also the least accurate by all measures compared to the other TSWs (Figure 7d). Most watersheds have the highest streamflow accuracy at 5 m; however, in P304, the 5 m resolution model failed to reproduce observed streamflow at an acceptable level (Equation (4)) > 0). In RHESys, surface topography is assumed to reflect the subsurface topography, but this assumption may not be valid in this watershed. Among TSWs, P304 with poor model performance has the highest summer flow rate [17], and shows different sediment load variability, sources and erosion rates than other TSWs [32].

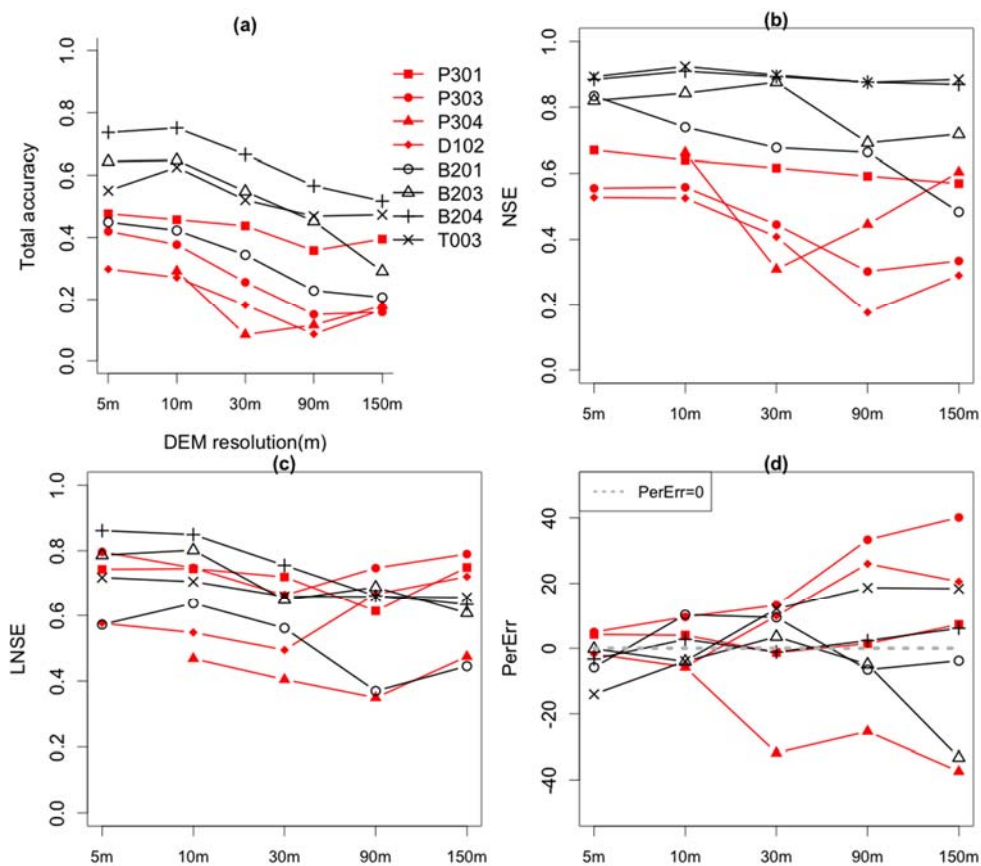


Figure 7. The model performance of streamflow prediction with different DEM resolutions. (a) total accuracy measure combining NSE, LNSE and PerErr; (b) NSE; (c) LNSE and (d) PerErr (percent error).

The 150 m resolution models for transient snow watersheds P301, P304 and D102 have higher accuracy than the 90 m resolution models. Similar results are observed for some SDWs where the 5 m resolution model has lower streamflow accuracy than the 10 m resolution model. Among SDWs, the streamflow accuracy for B201 is similar to those for TSWs, especially regarding the LNSE measure. NSE and LNSE for B201 are more sensitive to DEM resolution compared to the other watersheds. Other research [33] suggested that B201 has a smaller subsurface flow component than other Bull sites, and the authors hypothesized that the bedrock geomorphology at B201 may be different from the other watersheds. These results suggest that the model accuracy of streamflow depends on how well surface topography at different resolutions emulates the subsurface topography for individual watersheds. In addition to issues related to subsurface controls on streamflow, other unobserved differences in vegetation and drainage properties may have contributed to these differences in accuracy.

Since RHESy discretizes the watersheds based on DEM, and explicitly routes the flow and nutrient fluxes per grid or patch, increasing the DEM resolution will lead to increasing the computation running time. In our experiment, running times of the daily time step per year for T003, the largest watershed (2.3 km²), using a MacBook Pro (2.7 GHz Intel Core i5, 8 GB memory) were 1087 s (5 m), 621 s (10 m), 67 s (30 m), 7 s (90 m), 1 s (150 m). Therefore, the improved model results at 10 m require a longer time period to run the model than a scale of 30 m, but it still runs in 10 min which is very reasonable given the improvement.

4.3. Sensitivity of Estimated Ecohydrologic Variables to DEM Resolution

This study investigated how DEM resolution affects the long-term average ecohydrologic responses (annual flow, summer flow, annual ET, and annual NPP) to climate (Figure 8). Mean

annual streamflow estimates generally increase with coarser DEMs, especially for grid sizes that are coarser than 30 m. P304 and B203 are exceptions. T003 has the largest increase (44%) in mean annual flow, and B204 has the smallest increase (8%) in mean annual flow. Of the eco-hydrologic variables that we examined, mean summer flow is the most sensitive to DEM resolution, especially for SDWs, and generally increases with coarser DEMs. Among SDWs, T003 has the largest increase (150%) in mean summer flow with coarsening DEM. Among TSWs, P303 has the smallest decrease (21%) in mean summer flow. Mean annual ET values for SDWs are more sensitive to DEM resolution than TSWs. Coarsening the DEM reduces the mean annual ET. B201 has the largest change (33% decreases) in mean annual ET, and P301 has the smallest change (16% decreases) in mean annual ET. For most watersheds, coarsening DEM decreases the mean annual NPP. Compared with TSWs, mean annual NPP for SDWs is more sensitive to DEM resolution. T003 has the largest (50%) decrease in mean annual NPP, and P303 has smallest (14%) decrease in mean annual NPP.

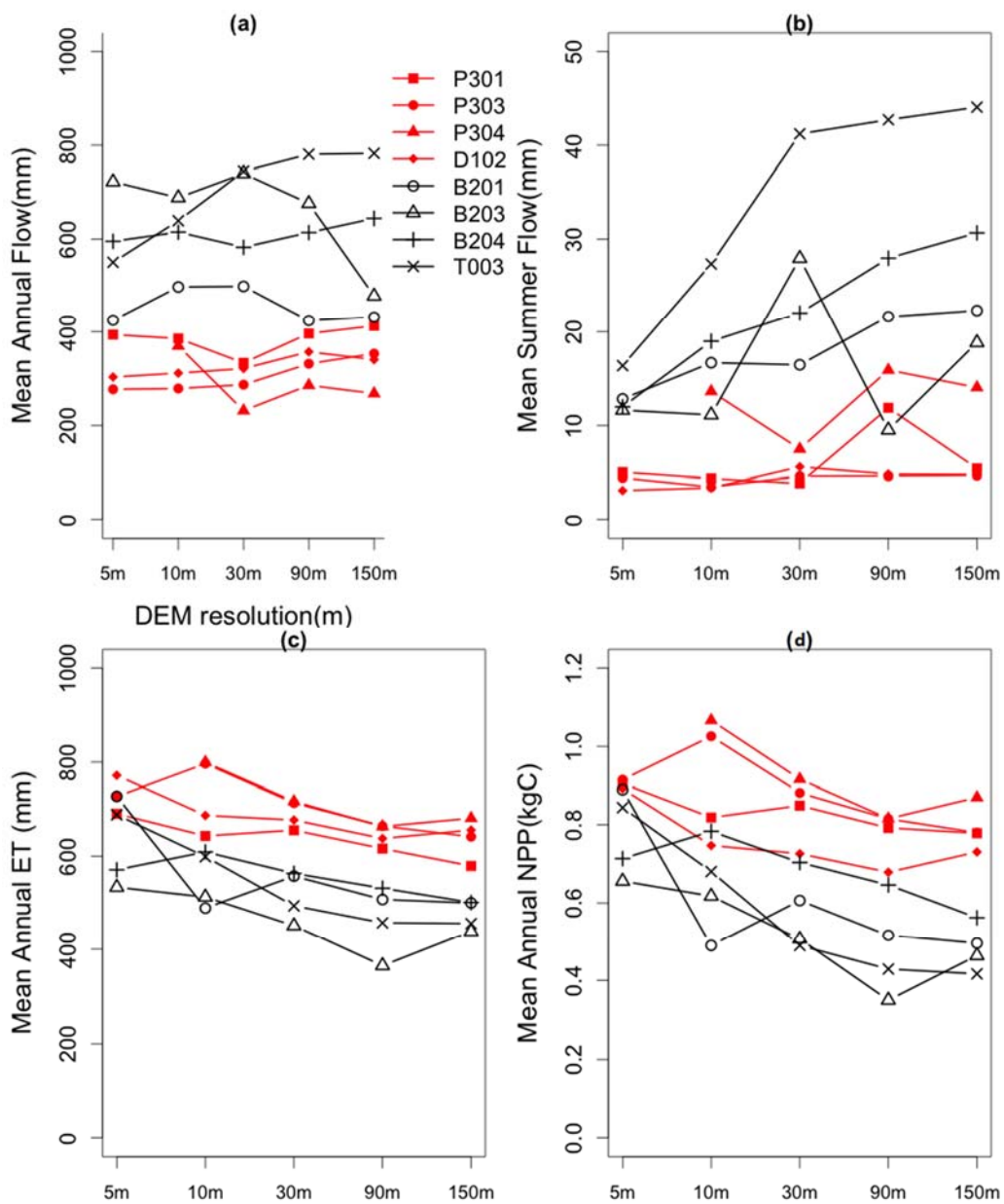


Figure 8. Annual mean of estimated ecohydrologic responses to climate with different DEM resolution. (a) mean annual flow; (b) mean summer (August) flow; (c) mean annual ET and (d) mean annual NPP.

We investigated the effect of DEM resolution on the sensitivity of each flux to inter-annual climate variation by calculating the COV at each resolution (Figure 9). TSWs tended to have a higher COV than SDWs for estimated annual streamflow, summer flow, annual ET, and annual NPP at 5 m. Coarsening the DEM has varied effects on the COVs among watersheds, and on the variables of interest. SDWs have higher changes in COV with the coarsening DEM resolution than TSWs. SDWs have larger increases in COV for annual NPP and larger decreases in COV for summer flow. There is not a large difference in the change of COV values for annual flow and annual ET between TSWs and SDWs. The COV values of annual NPP have the largest change with coarsening DEM, and the COV values of annual flow have the smallest change.

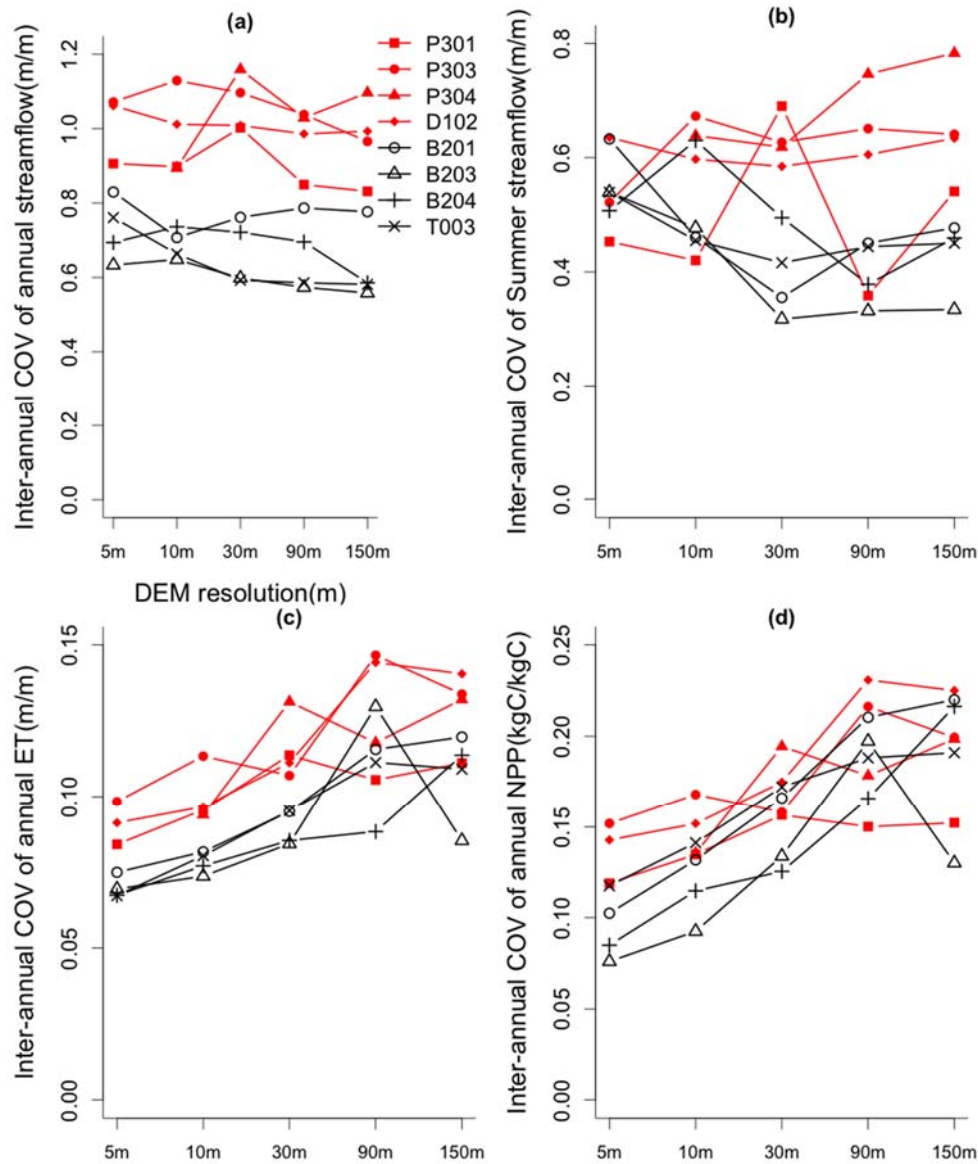


Figure 9. Inter-annual variability (coefficient of variance (COV)) of estimated ecohydrologic responses to climate with different DEM resolution (the variability was measured by coefficient of variance (COV)). (a) inter-annual streamflow variability; (b) inter-annual August streamflow variability; (c) inter-annual ET variability and (d) inter-annual NPP variability.

5. Discussion and Summary

This study was performed to improve our understanding of how DEM resolution affects ecohydrologic estimates in the context of using a model to evaluate climate change effects in small mountain watersheds. Three hypotheses were posed to test the DEM sensitivity within the TSW and SDW groups of watersheds and among the variables of interest: (1) model estimates for transient snow watersheds (TSWs) will have a higher sensitivity to DEM resolution than the model estimates for snow-dominated watersheds (SDWs); (2) changes in the spatial variation of the wetness index will explain the watershed sensitivity to DEM resolution; and (3) flow estimates will be more sensitive to DEM resolution than ET and NPP estimates.

This study showed that there is a clear threshold resolution (10 m) above which coarser resolutions have large effects on streamflow prediction accuracy (Figure 7). Among the eight watersheds, TSWs tend to have both a lower streamflow accuracy and a larger reduction of streamflow accuracy with coarsening DEM resolution (Table 3). Among TSWs, streamflow accuracy for P304 and D102 is the most sensitive to DEM resolution, but P301 is the second least-sensitive watershed to DEM resolution between the eight watersheds. The first hypothesis, that sensitivity to DEM resolution is closely linked to snow accumulation and melt characteristics, is not supported. The change in peak SWE with coarsening DEM is very minor for all eight watersheds. P301 with the lowest sensitivity to DEM resolution has the largest change in watershed absolute difference in SWE between 5 m and 150 m (Figure 5). Thus, the difference in the dominant precipitation phase between TSWs and SDWs does not lead to consistent differences in the sensitivity of flow estimates to changes in the model resolution.

Table 3. Watershed sensitivity to DEM resolution.

Watershed Group	Watershed	Change in Spatial Variance of Wetness Index (%)	Change in Streamflow Accuracy (Equation (4)) (%)	Model-Based Rank ⁵
TSWs	P301	−9 ¹ (3) ²	−25 ³ (−14) ⁴	7
	P303	−31 (−14)	−64 (−44)	3
	P304	−1 (5)	−71 (−42)	1
	D102	−26 (−11)	−71 (−41)	2
SDWs	B201	−5 (−1)	−54 (−33)	5
	B203	−4 (11)	−55 (−25)	4
	B204	7 (12)	−30 (−15)	6
	T003	11 (25)	−15 (−5)	8

Notes: ¹ The largest change in spatial variance of wetness index between the five resolution models; ² The mean change in spatial variance of wetness index between the five resolution models; ³ The largest change in streamflow accuracy between the five resolution models (Equation (4)); ⁴ The mean change in streamflow accuracy between the five resolution models (Equation (4)); ⁵ Ranked from highest to lowest sensitivity to DEM resolution, based on change in modeled streamflow accuracy.

Among topographic parameters, we hypothesized that the change in the spatial variation of the wetness index can explain the watershed sensitivity to DEM resolution. Changing the spatial variance of the wetness index has a complex relationship with coarsening DEM, and varies between watersheds. However, the lowering in the spatial variance of the wetness index with coarsening DEM corresponds with a reduction of the streamflow accuracy (Table 3). For example, when the 5 m resolution model was compared with coarser resolution models, P301 and D102 had the smallest reduction (−9%) and the largest reduction (−26%) of the spatial variance of the wetness index, respectively, which corresponds to the smallest and largest reductions of streamflow accuracy for the watersheds (−25% and −71%, respectively). Among the eight watersheds, T003 has the smallest reduction (−15%) of the streamflow accuracy, and that watershed shows an increase (11%) of the spatial variance of the wetness index. RHESys does not use the wetness index directly to calculate lateral flow. However, the wetness index includes the component of topographic slope and flow-accumulating area. RHESys actually uses these components to determine the lateral flow paths. Previous studies using TOPMODEL [10] also showed that decreasing resolution reduces the spatial variance of the wetness index [6,34]. Pradhan et al. [34]

showed that when a coarser DEM resolution (1000 m) reproduced the cumulative distribution of the wetness index at the fine resolution (50 m), the streamflow estimates using the coarser 1000 m DEM resolution matched the simulated streamflow in the 50 m DEM resolution TOPMODEL without recalibration. Results in this study suggest that the change in the wetness index distribution will also be a good indicator of whether coarsening the DEM will lead to reduced accuracy for an explicit routing model. Kenward et al. [31] tested the impact of DEM resolution on the streamflow accuracy and spatial pattern of a predicted saturated area using DHSVM [35] which has a similar routing scheme to RHESys. Their study also showed that the spatial distribution of the wetness index corresponded to the depth to saturation and runoff production for a rain-dominated system in the WF-38 experimental watershed at the Mathantango Creak, PA. Our study confirms that the impact of DEM resolution on flow paths is also likely to be important for snow and rain-snow transition watersheds and that the impact of model resolution on the lateral redistribution of water may be more important than its impact on snow accumulation and melt for models of low-order, headwater watersheds.

Among the model accuracy measures, PerErr has the highest sensitivity to DEM resolution. Changes in PerErr are directly related to changes in annual ET. We note that annual ET estimates and their COV are strongly sensitive to DEM resolution (Figures 8 and 9). Changes in the wetness index distribution may also be important in ET estimates, particularly in water-limited environments. The impact of DEM resolution on ET is discussed in more detail below.

Among the model estimates, we hypothesized that the flow estimate to DEM resolution will be more sensitive than ET and NPP estimates. Our modeling results found that among the four ecohydrologic estimates of interest, DEM resolution has the largest effects on the mean summer flow and COV of the annual ET and NPP (Figures 7 and 8). One of the eight watersheds, T003 had the smallest reduction in streamflow accuracy with coarsening DEM, but large changes in the mean summer flow (150%), the COV of the annual ET (65%), and the COV of the annual NPP (60%) are observed. These results emphasize that accurate streamflow prediction does not guarantee a model's ability to capture long-term ecohydrologic responses to climate change. Our study also suggests that using a fine-resolution DEM in ecohydrologic modeling is essential in order to capture the long-term observed summer flow. Since summer flow is an important water resource and has substantial implications for aquatic organisms in California, fine-scale hydrologic modeling for assessing the effect of climate change in Sierra Nevada is necessary [36].

Our modeling study showed that a coarsening DEM resolution results in an increase in the COV of both ET and NPP. This result implies that coarser-resolution models overestimate the sensitivity of these processes to climate variation. This result is important for interpreting and predicting ecosystem responses to climate change. The reduced sensitivity of ET and NPP for the finer-resolution models may be related to the substantial variation in topographic properties in mountain environments. The high variation in topographic properties may lead to spatial variation in the sizes of water storage and flow path convergence. As discussed above, coarsening the DEM tends to reduce spatial variation in the wetness index. The vegetation response to changing climate may be lower for the finer-resolution model because this spatial variation in water storage and flow path convergence provides additional opportunities for plants to access water. A higher-resolution DEM, for example, may lead to greater areas of local flow path convergence typified by riparian areas and local depressions with greater soil moisture. ET in these areas may be less sensitive to inter-annual climate variation. The higher COV of ET and NPP with coarsening DEM resolution may also illustrate the role of micro-refuge created by substantial variation in other topographic properties in mountain environments [37]. Dobrowski et al. [37] provide case studies where terrain allows for local climate conditions to be decoupled from the regional climate; when sites decouple from the regional climate, micro-refuges can occur for species. The finer-resolution model may create microclimate conditions, as well as areas of increased moisture storage, that are less sensitive to the forcing climate variability.

In summary, this study demonstrates that using fine-scale DEM in ecohydrologic modeling influences the accuracy of streamflow estimation in headwater mountain catchments and substantially

alters estimates of climate-driven inter-annual variation in ET and NPP in these systems. Results emphasize that these effects may be largely due to the role of the DEM in the model estimation of hydrologic flowpaths rather than the model estimation of snow accumulation and melt. This study found that coarser-resolution models tend to have lower streamflow accuracy and overestimate climate sensitivity for ET and NPP. These results have important implications for model-based studies used to assess ecosystem responses to climate change, and, in particular, caution that coarser-resolution models may overestimate climate sensitivity. The analysis, however, demonstrates a non-linear relationship between model accuracy/sensitivity and DEM resolution and suggests that increasing resolution from 30 m to 10 m makes substantial improvements. Further increasing the resolution to 5 m results in smaller gains in performance, relative to the increase in computation cost.

Acknowledgments: We gratefully acknowledge the data collected by Kings River Experimental Watershed Project (KREW) and this study was financially supported by Southern Sierra Critical Zone Observatory Project from National Science Foundation (EAR-0725097).

Author Contributions: Kyongho Son performed the data processing and modeling and wrote the manuscript, and Christina Tague helped the RHESSys model setup, and revised the manuscript and analyzed and interpreted the modeling results. Carlyon Hunsaker provided the basic hydrologic data used in this study, and helped improve the structure and language of the manuscript.

Conflicts of Interest: The authors declare no conflict of interest.

References

1. Knowles, N.; Cayan, D.R. Potential effects of global warming on the Sacramento/San Joaquin watershed and the San Francisco estuary. *Geophys. Res. Lett.* **2002**, *29*, 1891. [[CrossRef](#)]
2. Maurer, E.; Duffy, P.P.B. Uncertainty in projections of streamflow changes due to climate change in California. *Geophys. Res. Lett.* **2005**, *32*, L03704. [[CrossRef](#)]
3. Goulden, M.L.; Bales, R.C. Mountain runoff vulnerability to increased evapotranspiration with vegetation expansion. *Proc. Natl. Acad. Sci. USA* **2014**, *111*, 14071–14075. [[CrossRef](#)] [[PubMed](#)]
4. Miller, N.L.; Bashford, K.E.; Strem, E. Potential impacts of climate change on California hydrology. *J. Am. Water Resour. Assoc.* **2003**, *39*, 771–784. [[CrossRef](#)]
5. Null, S.E.; Viers, J.H.; Mount, J.F. Hydrologic response and watershed sensitivity to climate warming in California's Sierra Nevada. *PLoS ONE* **2010**, *5*, e9932. [[CrossRef](#)] [[PubMed](#)]
6. Zhang, W.; Montgomery, D.R. Digital elevation model grid size, landscape representation, and hydrologic simulations. *Water Resour. Res.* **1994**, *30*, 1019–1028. [[CrossRef](#)]
7. Cline, D.; Elder, K.; Bales, R. Scale effects in a distributed snow water equivalence and snowmelt model for mountain basins. *Hydrol. Process.* **1998**, *1536*, 1527–1536. [[CrossRef](#)]
8. Lassueur, T.; Joost, S.; Randin, C.F. Very high resolution digital elevation models: Do they improve models of plant species distribution? *Ecol. Model.* **2006**, *198*, 139–153. [[CrossRef](#)]
9. Beven, K.J.; Kirkby, M.J. A physically based, variable contributing area model of basin hydrology/Un modèle à base physique de zone d'appel variable de l'hydrologie du bassin versant. *Hydrol. Sci. Bull.* **1979**, *24*, 43–69. [[CrossRef](#)]
10. Kuo, W.; Steenhuis, T.S.; Mcculloch, C.E.; Mohler, C.L.; Weinstein, D.A.; DeGloria, S.D.; Swaney, D.P. Effect of grid size on runoff and soil moisture for a variable-source-area hydrology model. *Water Resour. Res.* **1999**, *35*, 3419–3428. [[CrossRef](#)]
11. Musselman, K.N.; Molotch, N.P.; Brooks, P.D. Effects of vegetation on snow accumulation and ablation in a mid-latitude sub-alpine forest. *Hydrol. Process.* **2008**, *22*, 2767–2776. [[CrossRef](#)]
12. Jost, G.; Weiler, M.; Gluns, D.R.; Alila, Y. The influence of forest and topography on snow accumulation and melt at the watershed-scale. *J. Hydrol.* **2007**, *347*, 101–115. [[CrossRef](#)]
13. Chaubey, I.; Cotter, A.S.; Costello, T.A.; Soerens, T.S. Effect of DEM data resolution on SWAT output uncertainty. *Hydrol. Process.* **2005**, *19*, 621–628. [[CrossRef](#)]
14. Mahmood, T.H.; Vivoni, E.R. Breakdown of hydrologic patterns upon model coarsening at hillslope scales and implications for experimental design. *J. Hydrol.* **2011**, *411*, 309–321. [[CrossRef](#)]

15. Mo, X.; Liu, S.; Chen, D.; Lin, Z.; Guo, R.; Wang, K. Grid-size effects on estimation of evapotranspiration and gross primary production over a large Loess Plateau basin, China. *Hydrol. Sci. J.* **2009**, *54*, 160–173. [[CrossRef](#)]
16. Tague, C.L.; Band, L.E. RHESSys: Regional hydro-ecologic simulation system—An object-oriented approach to spatially distributed modeling of carbon, water, and nutrient cycling. *Earth Interact.* **2004**, *8*, 1–42. [[CrossRef](#)]
17. Hunsaker, C.T.; Whitaker, T.W.; Bales, R.C. Snowmelt runoff and water yield along elevation and temperature gradients in California’s Southern Sierra Nevada. *JAWRA J. Am. Water Resour. Assoc.* **2012**, *48*, 667–678. [[CrossRef](#)]
18. Jefferson, A.J. Seasonal versus transient snow and the elevation dependence of climate sensitivity in maritime mountainous regions. *Geophys. Res. Lett.* **2011**, *38*. [[CrossRef](#)]
19. Holmgren, P. Multiple flow direction algorithms for runoff modelling in grid based elevation models: An empirical evaluation. *Hydrol. Process.* **1994**, *8*, 327–334. [[CrossRef](#)]
20. Running, S.W.; Nemani, R.R.; Hungerford, R.D. Extrapolation of synoptic meteorological data in mountainous terrain and its use for simulating forest evapotranspiration and photosynthesis. *Can. J. For. Res.* **1987**, *17*, 472–483. [[CrossRef](#)]
21. Glassy, J.; Running, S. Validating diurnal climatology logic of the MT-CLIM model across a climatic gradient in Oregon. *Ecol. Appl.* **1994**, *4*, 248–257. [[CrossRef](#)]
22. Coughlan, J.; Running, S. Regional ecosystem simulation: A general model for simulating snow accumulation and melt in mountainous terrain. *Landsc. Ecol.* **1997**, *12*, 119–136. [[CrossRef](#)]
23. Thornton, P.E.; Running, S.W.; White, M.A. Generating surfaces of daily meteorological variables over large regions of complex terrain. *J. Hydrol.* **1997**, *190*, 214–251. [[CrossRef](#)]
24. Monteith, J.L. Evaporation and environment. *Symp. Soc. Exp. Biol.* **1965**, *19*, 205–234. [[PubMed](#)]
25. Jarvis, P.G. The interpretation of the variations in leaf water potential and stomatal conductance found in canopies in the field. *Philos. Trans. R. Soc. B Biol. Sci.* **1976**, *273*, 593–610. [[CrossRef](#)]
26. Farquhar, G.D.; von Caemmerer, S.; Berry, J.A. A biochemical model of photosynthetic CO₂ assimilation in leaves of C₃ species. *Planta* **1980**, *149*, 78–90. [[CrossRef](#)] [[PubMed](#)]
27. Ryan, M.G. Effects of climate change on plant respiration. *Ecol. Appl.* **1991**, *1*, 157–167. [[CrossRef](#)]
28. Richardson, J.J.; Moskal, L.M.; Kim, S.-H. Modeling approaches to estimate effective leaf area index from aerial discrete-return LIDAR. *Agric. For. Meteorol.* **2009**, *149*, 1152–1160. [[CrossRef](#)]
29. Dunn, S.M. Imposing constraints on parameter values of a conceptual hydrological model using baseflow response. *Hydrol. Earth Syst. Sci.* **1999**, *3*, 271–284. [[CrossRef](#)]
30. Nash, J.E.; Sutcliffe, J.V. River flow forecasting through conceptual models part I—A discussion of principles. *J. Hydrol.* **1970**, *10*, 282–290. [[CrossRef](#)]
31. Kenward, T.; Lettenmaier, D.P.; Wood, E.F.; Fielding, E. Effects of digital elevation model accuracy on hydrologic predictions. *Remote Sens. Environ.* **2000**, *444*, 432–444. [[CrossRef](#)]
32. Hunsaker, C.; Neary, D. Sediment loads and erosion in forest headwater streams of the Sierra Nevada, California. In Proceedings of a Workshop Held during the XXV IUGG General Assembly in Melbourne, Melbourne, Australia, 28 June–7 July 2011.
33. Liu, F.; Hunsaker, C.; Bales, R.C. Controls of streamflow generation in small catchments across the snow-rain transition in the Southern Sierra Nevada, California. *Hydrol. Process.* **2013**, *12*, 1959–1972. [[CrossRef](#)]
34. Pradhan, N.R.; Ogden, F.L.; Tachikawa, Y.; Takara, K. Scaling of slope, upslope area, and soil water deficit: Implications for transferability and regionalization in topographic index modeling. *Water Resour. Res.* **2008**, *44*. [[CrossRef](#)]
35. Wigmosta, M.S.; Vail, L.W.; Lettenmaier, D.P. A distributed hydrology-vegetation model for complex terrain. *Water Resour. Res.* **1994**, *30*, 1665–1679. [[CrossRef](#)]
36. Tague, C.; Dugger, A. Ecohydrology and climate change in the mountains of the Western USA—A review of research and opportunities. *Geogr. Compass* **2010**, *11*, 1648–1663. [[CrossRef](#)]
37. Dobrowski, S.Z. A climatic basis for microrefugia: the influence of terrain on climate. *Glob. Chang. Biol.* **2011**, *17*, 1022–1035. [[CrossRef](#)]

